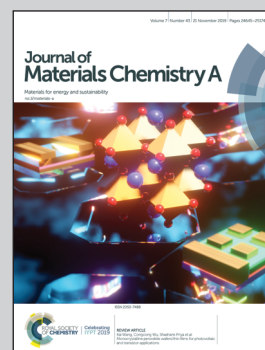


A new concept of an auxiliary electrode that is capable of sensing and retarding the lithium dendrite growth in lithium metal electrodes. This advance sensor has been well developed by a group of researchers led by Sehwan Moon and Orapa Tamwattana from Seoul National University, Asst. Prof. Nonglak Meethong from Khon Kaen University and Prof. Kisuk Kang from Seoul National University.

A bifunctional auxiliary electrode for safe lithium metal batteries

A bifunctional auxiliary electrode is a new concept of the active safety sensor, which not only detects the internal electrical short but also plays a role of lithium scavenging agent. It is demonstrated that the bifunctional auxiliary electrode with such functions successfully detects signals of a short-circuit hazard and inhibits further dendrite growth, with a minimal sacrifice in the energy density. This advance sensor opens up unexplored pathways of using various auxiliary electrode chemistry toward the development of practical lithium metal batteries.



As featured in:



See Nonglak Meethong,  
Kisuk Kang *et al.*,  
*J. Mater. Chem. A*, 2019, 7, 24807.

Cite this: *J. Mater. Chem. A*, 2019, 7, 24807

## A bifunctional auxiliary electrode for safe lithium metal batteries†

Sehwan Moon,<sup>‡a</sup> Orapa Tamwattana,<sup>‡ab</sup> Hyeokjun Park,<sup>ac</sup> Gabin Yoon,<sup>ac</sup> Won Mo Seong,<sup>a</sup> Myeong Hwan Lee,<sup>a</sup> Kyu-Young Park,<sup>a</sup> Nonglak Meethong <sup>\*de</sup> and Kisuk Kang <sup>\*ac</sup>

Increasing demands for performance beyond the limit of current lithium ion batteries for higher energy densities have rejuvenated research using lithium metal as an anode. However, commercial implementation has still been hampered due to safety issues. Herein, we introduce a lithium rechargeable battery system with an auxiliary electrode that can detect the potential signs of an internal short-circuit and simultaneously prevent cell failure by inhibiting further dendritic growth of lithium metal. Based on this working principle, we provide guidelines for an auxiliary electrode design and demonstrate that it can act as both a safety sensor and a lithium scavenger. Finally, we show that our in-house designed cell, using a flexible and self-standing auxiliary electrode, can effectively alert the danger of a short circuit in real-time without additional dendrite growth. We expect that this finding will open up unexplored opportunities utilizing various auxiliary electrode chemistries for safe rechargeable lithium metal batteries.

Received 24th July 2019  
Accepted 19th August 2019

DOI: 10.1039/c9ta08032e

rsc.li/materials-a

### Introduction

The demand for rechargeable batteries with higher energy density than lithium ion batteries that are commercially available has been ever increasing.<sup>1,2</sup> Elemental lithium metal has thus come into the spotlight again as one of the most promising negative electrode materials owing to its exceptionally high theoretical capacity (3860 mA h g<sup>-1</sup>) and the lowest negative electrochemical potential (−3.040 V vs. a standard hydrogen electrode).<sup>3,4</sup> However, the commercialization of rechargeable lithium metal batteries (LMBs) has been retarded due to the catastrophic safety issue arising from lithium dendrite formation. Even with a small irregularity in lithium metal deposition during the initial stage of charge, further selective and self-

amplifying lithium deposition occurs due to the presence of favorable deposition sites. The inhomogeneous lithium deposition depending on operating conditions leads to the formation of dendrites in a variety of morphologies such as filamentary, mossy or fork-like shapes, which is related to the possibility of short circuit phenomena.<sup>5–7</sup> The needle-like lithium dendrite can penetrate the polymer separator and possibly come into contact with the opposite electrode, and such contact would result in a huge current flow through the internal circuit, triggering joule heating thermal runaway.<sup>8,9</sup>

Over the last few decades, tremendous efforts have been focused on elucidating the dendritic growth mechanism<sup>10,11</sup> and preventing lithium dendrite formation. Although much progress has been made in understanding the lithium dendritic growth, the development of reliable techniques for controlling the surface morphology from heterogeneous reactions still remains an obstacle. Various attempts such as introduction of electrolyte additives<sup>12–14</sup> to avoid undesirable reactions at the lithium surface and a three-dimension current collector<sup>15,16</sup> to induce uniform reactions and a physically protective layer have been explored.<sup>17,18</sup> Unfortunately, it has been revealed that the dendrite formation cannot be completely inhibited and such approaches are only valid at low current densities and/or with a low utilization level of lithium metal anodes. Batteries operating under extreme conditions might still be exposed to the potential risk of dendrite growth and the internal short-circuit. Therefore, not only protective techniques for lithium metal, but also sensing technologies to detect dendritic growth in advance are needed. Recently, Wu *et al.* reported an early detection

<sup>a</sup>Department of Materials Science and Engineering, Research Institute for Advanced Materials, College of Engineering, Seoul National University, 1 Gwanak-ro, Gwanak-gu, Seoul 151-742, Republic of Korea. E-mail: matlgen1@snu.ac.kr

<sup>b</sup>Institute of Nanomaterials Research and Innovation for Energy (IN-RIE), Department of Physics, Faculty of Science, Khon Kaen University, Muang Khon Kaen, Thailand 40002

<sup>c</sup>Center for Nanoparticle Research at Institute for Basic Science (IBS), Seoul National University, 1 Gwanak-ro, Gwanak-gu, Seoul 151-742, Republic of Korea

<sup>d</sup>Institute of Nanomaterials Research and Innovation for Energy (IN-RIE), Research Network of NANOTEC-KKU (RNN), Khon Kaen University, Muang Khon Kaen, Khon Kaen, Thailand. E-mail: nonmee@kku.ac.th

<sup>e</sup>Materials Science and Nanotechnology Program, Department of Physics, Faculty of Science, Khon Kaen University, Muang Khon Kaen, Thailand

† Electronic supplementary information (ESI) available. See DOI: 10.1039/c9ta08032e

‡ These authors contributed equally to this work.

technique, where metallic copper was sputtered on a separator to detect the electrical shortage caused by lithium metal penetration through the separator.<sup>19</sup> The bifunctional separator could successfully detect the internal short circuit when the lithium dendrite penetrated into the separator, enabling the alarming of the cell failure. Nevertheless, it is questionable whether this early detection would be practically linked to the prevention of the actual cell failure in consideration of the typical dendrite growth rate ( $5.1 \mu\text{m s}^{-1}$  at a current density  $50 \text{ mA cm}^{-2}$ , ESI Fig. S1†). The detection of the shortage means that the lithium has already substantially grown and is at the risk of coming into contact with the counter electrode, having passed through the separator. As the thickness of the conventional separator is  $<12 \mu\text{m}$ , the time from the sensing to the potential safety hazard is only less than a few seconds. Moreover, at higher current rates for fast charging or discharging, the detection would not simply offer a sufficient time to stop the catastrophic reaction.

Herein, we explored a more advanced concept of a safety sensor, which not only detects an internal electrical short, but also plays the role of a lithium scavenging agent. In this concept, an auxiliary electrode signals an internal short-circuit in real-time, and upon the short-circuiting of the battery, it scavenges a certain amount of lithium, preventing further growth of dendrites, allowing enough time to shut down the circuit without incurring a safety hazard.

## Working principle and auxiliary electrode design

The working principle of an auxiliary electrode in sensing and scavenging is schematically illustrated in Fig. 1, where an auxiliary electrode is inserted between the positive and negative electrodes. In the absence of an auxiliary electrode, the unwanted dendrite growth from the lithium surface eventually

reaches the positive electrode, which potentially serves as an electron pathway with very low resistance. A large amount of electrons, driven by the potential difference between two electrodes, will pass through this pathway in an uncontrolled manner within a short time and can possibly cause a thermal runaway due to the heat generated by the high current. This phenomenon is indicated by the near '0' voltage in the voltmeter shown in Fig. 1a. In contrast, a real-time detection of dendrite growth can be achieved by inserting an auxiliary electrode between the separators (Fig. 1b).<sup>19</sup> Using this cell configuration, the auxiliary electrode is designed to physically come into contact with a growing lithium metal dendrite before it reaches the positive electrode. Upon contact, a voltage change would be detected between the negative and the auxiliary electrodes (Fig. 1b) and this gives a warning signal to the battery user in real-time. Moreover, in our design of the bifunctional auxiliary electrode, it was intended that it should also be capable of taking up a certain amount of lithium, so that further development of dendrite growth toward the positive electrode can be inhibited for some time, achieving a partial self-healing with safety detection.

For this aim, the material for an auxiliary electrode should be carefully selected and machined to fulfill the following requirements: (i) it should be capable of spontaneously accepting lithium ions from lithium metal ( $\mu_{\text{auxiliary electrode}} < \mu_{\text{Li metal}}$ ;  $\mu$  refers to the chemical potential of lithium) with a reasonably fast rate. (ii) The physical contact between the auxiliary electrode and dendrites should be easily recognizable. (iii) The capacity of the auxiliary electrode must be reliably determined, so that the amount of allowable lithium uptake and the data collection interval in the system can be verified. (iv) The auxiliary electrode should not undergo a large volume change upon lithiation and not interfere with the movement of lithium ions. Taking all these requirements into consideration, we selected free-standing, flexible and thin graphite layers and

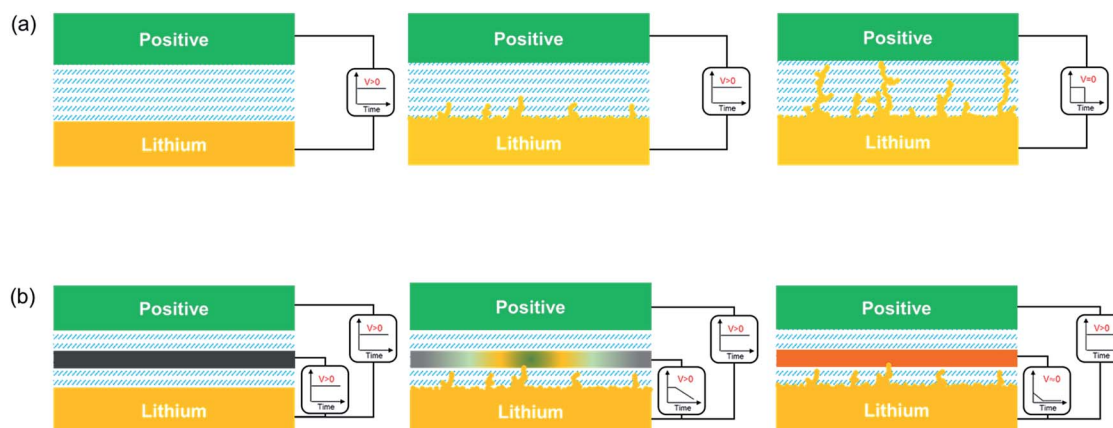


**Fig. 1** Schematic mechanism of an auxiliary electrode sensor for safe rechargeable lithium metal batteries. (a) In a conventional battery system, initially formed dendritic seeds will grow and create an internal circuit across the separator positioned between the two electrodes, causing the voltage of the battery to drop to 0 V (vs.  $\text{Li}/\text{Li}^+$ ). (b) With the aid of the auxiliary electrode, growing lithium dendrites will reach the auxiliary electrode before they make connection with the positive electrode. Lithium dendrites will not grow further while the auxiliary electrode consumes lithium ions. The reaction of the auxiliary electrode with lithium ions signals danger before a catastrophic event occurs with no damage to the battery.

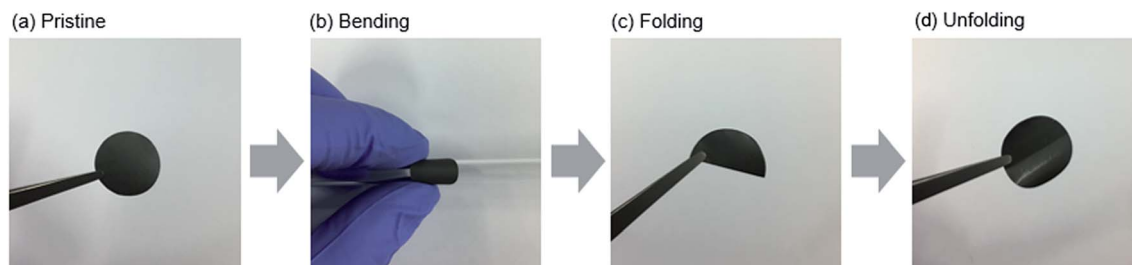


Fig. 2 Images of a flexible graphite layer with 30% PVDF–HFP and 70% flake graphite composition. (a) Pristine, (b) bending, (c) folding and (d) unfolding of graphite layer. The pristine graphite layer was not torn and damaged by bending and folding.

prepared them as described in Fig. 2 and S2.† Graphite is well-known to be capable of taking up lithium ions at a reasonably fast rate, with its capacity well-documented.<sup>20</sup> Moreover, the degree of lithiation is clearly observable from 3 V to nearly 0 V with the well-defined voltage plateau and a color change of graphite (ESI Fig. S3†).<sup>21,22</sup> In this work, the free-standing film of graphite was fabricated using poly(vinylidene fluoride-co-hexafluoropropylene) (PVDF–HFP) with the mass ratio of 3 : 7 (PVDF–HFP : graphite) with 20  $\mu\text{m}$  thickness, considering the reasonable holding time of lithium growth at various current rates in a practical cell as presented in ESI Fig. S4.† It should be also noted that such a thin free-standing auxiliary graphite electrode still guarantees much higher gravimetric and volumetric energy density of the lithium metal anode in spite of the additional weight of the auxiliary electrodes, as comparatively demonstrated in ESI Tables S1 and S2.† The electrolyte permeability of the thin layer was confirmed through a simple dropping test of the electrolyte. The images in ESI Fig. S5† show that the fabricated flexible graphite layer has better wettability than the separator.<sup>23,24</sup> The effect of the auxiliary electrode on lithium ion mobility in the cell was quantitatively analyzed using electrochemical impedance spectroscopy (ESI Fig. S6†).<sup>25</sup> The influence of the auxiliary graphite layer on the ionic conductivity in the cell was negligible with a decrease of 0.12  $\text{mS cm}^{-1}$ .

## Experimental

The detailed function of an auxiliary electrode was verified through *in situ* observations of dendrite growth in the lithium metal cell. We prepared a home-made lithium cell to enable capture of images of dendrite growth while measuring the auxiliary electrode potential, as illustrated in Fig. 3a. Voltage profiles,  $V_1$  (between lithium and copper) and  $V_2$  (between lithium and the auxiliary electrode) were simultaneously monitored. Initially, the measured voltages,  $V_1$  and  $V_2$ , were 0 V and  $\sim 3$  V, respectively, presenting an initial potential difference between the two electrodes. As soon as the current was applied, it was observed that lithium ions began to deposit on the copper, and  $V_1$  rapidly fell below 0 V ( $\sim -0.8$  V) due to the overpotential. However,  $V_2$  remained almost unchanged from the initial voltage at nearly 3 V because the graphite layer is disconnected from the electric circuit. Fig. 3b shows that, with the continuous current flow in the circuit, the lithium metal

deposits irregularly on the surface of the copper foil and finally comes into contact with the auxiliary graphite layer after about 10 minutes. It is evident from Fig. 3c that, at the moment of the contact between the lithium metal protrusion and the auxiliary electrode, a sudden voltage drop of  $V_2$  can be observed, while a small voltage change of  $V_1$  is detected (this will be discussed in detail later), which is in contrast to a system without the auxiliary electrode<sup>26</sup> as shown in ESI Fig. S7.† The change of  $V_2$  is ascribed to the gradual lithium intercalation into the graphite auxiliary electrode, which alters the lithium chemical potential in the auxiliary electrode, thus the potential difference between the two electrodes. This implies that the lithium gradually intercalates into the auxiliary electrode. However, it is worth noting that the lithium intercalation into graphite can take place from both of the lithium sources once the lithium protrusions are in electrical contact with the graphite layer: (i) chemical lithiation from the lithium protrusions and (ii) partial electrochemical lithiation from the lithium metal electrode through the electrolyte. Since the graphite layer becomes a part of the electric circuit, the electrochemical lithiation into graphite becomes possible, which is thermodynamically preferable than being electroplated as lithium metal on the lithium metal electrode. These two processes simultaneously contribute to suppressing the further growth of lithium protrusion. The chemical lithiation into graphite from the lithium protrusion scavenges the protrusion itself, and the further lithium deposition on the lithium metal electrode is temporarily halted by the electrochemical lithiation of the graphite layer.

More careful investigation of the  $V_1$  and  $V_2$  profiles supports the idea that the auxiliary electrode played the role of a lithium dendrite scavenger. Fig. 3d depicts the detailed voltage evolutions of  $V_1$  and  $V_2$  during the initial a few minutes after the contact, showing a close correlation between the two, while  $V_2$  continues to drop to 0 V for this period of time, slight perturbations appear intermittently for both  $V_1$  and  $V_2$ . And, it is noteworthy that the peak in the  $V_1$  profile coincides with the step-wise drop of  $V_2$ . We believe that this is due to the repeated formation and removal of dendrites, forming and breaking an electric circuit. After the first contact resulting from the formation of the dendrite, there is an instantaneous drop in  $V_2$  followed by a small peak at 10.7 minutes marked as the black star in Fig. 3d (*i.e.* the instantaneous reduction in the overpotential of  $V_1$ ) for  $V_1$ . And, at 11.2 and 11.45 minutes marked as black stars in Fig. 3d, the small peaks in  $V_1$  are accompanied



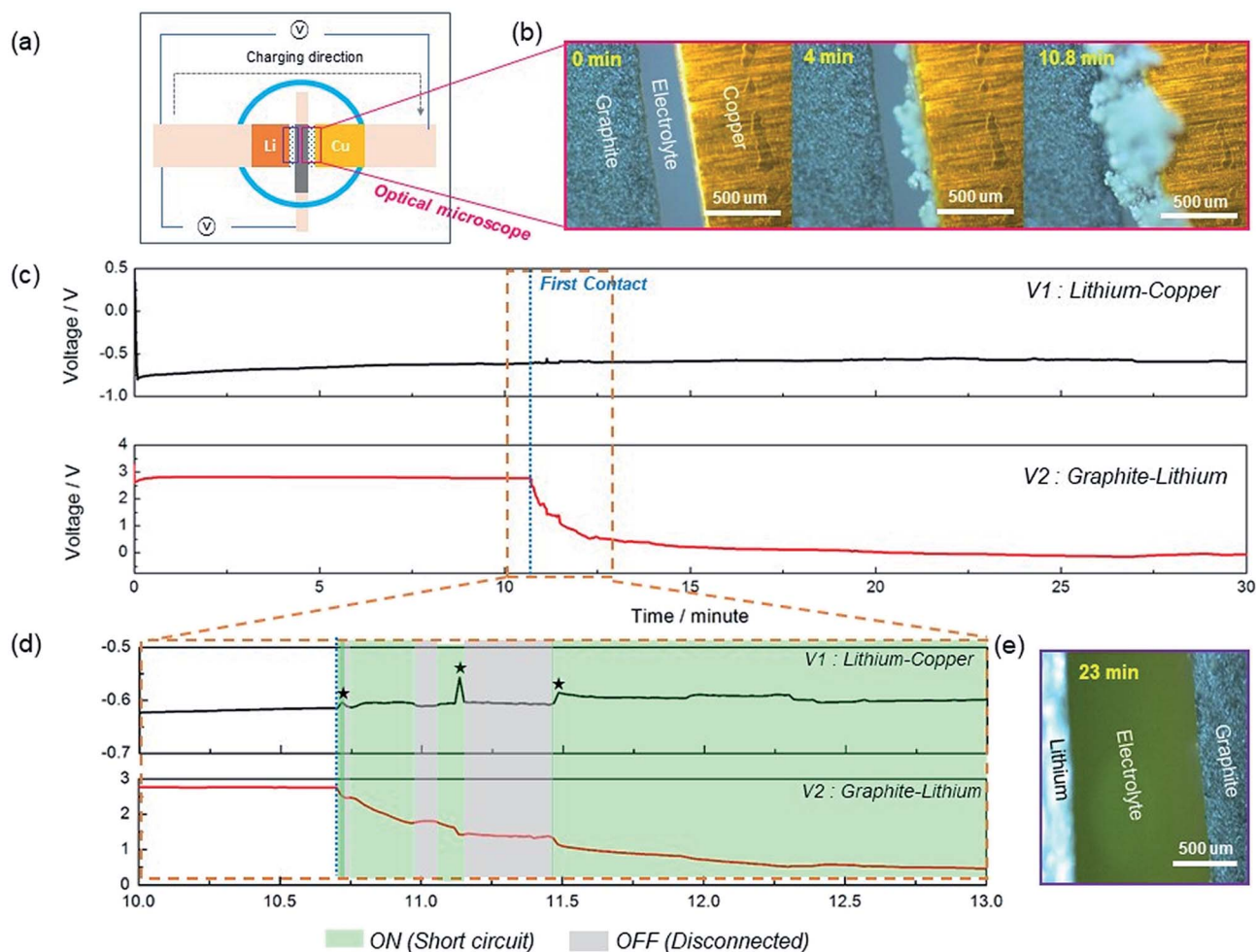


Fig. 3 (a) Detailed cell configuration for *in situ* observations. (b) Images of the auxiliary electrode and positive electrode were taken over deposition time. Mossy-like lithium was observed on the copper foil that gradually grew over time. (c) The voltage profile of both  $V_{1\text{Lithium-Copper}}$  and  $V_{2\text{Graphite-Lithium}}$  during electroplating on copper foil. (d)  $V_{1\text{Lithium-Copper}}$  and  $V_{2\text{Graphite-Lithium}}$  from 10 to 13 minutes. (e) Images of the area between the auxiliary electrode and negative electrode after 23 minutes. No trace of lithium deposition was observed, indicating that the mossy-like lithium did not penetrate the graphite layer.

by the faster decrease of the  $V_2$  voltage. The decrease of the overpotential in  $V_1$  upon the contact is likely to be caused by the reduction in the effective anode-cathode distance owing to the electrical contact.<sup>27</sup> And, if more dendrites are generated penetrating into the auxiliary electrode, they provide additional electronic bridges by which electrons can pass, resulting in a further decrease of the overpotential in  $V_1$  and faster lithium intercalation into graphite (more rapid reduction in  $V_2$  voltage), as presented with green colors in Fig. 3d.

On the other hand, if the dendrites are consumed by the chemical lithiation and thus are removed from the auxiliary electrode, the overpotential in  $V_1$  would reappear, as illustrated with grey regions in Fig. 3d. This scavenger role of the auxiliary electrode continued until it was completely lithiated, which is further supported by the additional *ex situ* and *in situ* Li-Li symmetric cell results in ESI Fig. S8 and Video 1.† It should be noted that, as a result, there was no dendritic lithium penetration to the opposing lithium electrode even after 23 minutes of constant discharging (Fig. 3e).

The results above indicate that not only  $V_2$  but also  $V_1$  is notably altered, when the dendrite comes in contact with the auxiliary electrode even though there is no electrical shorting between the positive electrode and negative electrode. This implies that in a conventional cell without an additional apparatus to monitor the  $V_2$ , it might be simply possible to detect the dendrite signal from the change in the nominal voltage ( $V_1$ ) of the cell when the auxiliary electrode begins to scavenge them. To verify this, we assembled a conventional coin-type cell without an apparatus monitoring  $V_2$  and tested the cell at a practically high current rate using a lithium metal negative electrode and a graphite positive electrode, as shown in Fig. 4a. The graphite was chosen as a model positive electrode because its characteristic voltage profile is well documented with a minimum variation of the specific capacity at a given voltage range, which is beneficial for monitoring the distinctive voltage changes in the cell. We first discharged the cell at a low current density of  $10\text{ mA g}^{-1}$ , *i.e.* lithiation of the graphite positive electrode and stripping of the lithium metal negative

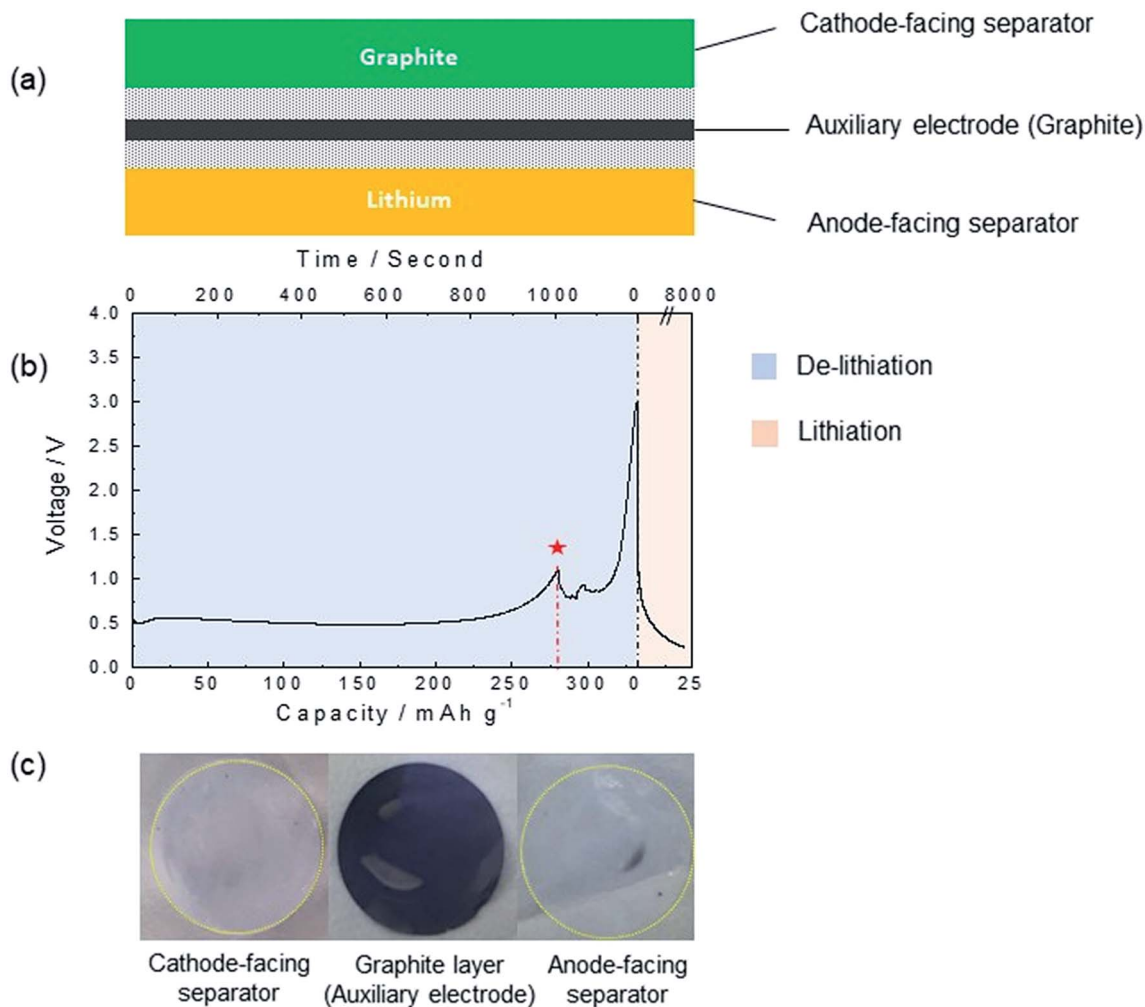


Fig. 4 (a) Schematic of the cell configuration. (b) The first charge voltage profile with a  $1000 \text{ mA g}^{-1}$  current density and a second charge voltage profile with a  $10 \text{ mA g}^{-1}$  current density. (c) Images of separators and auxiliary electrodes from a disassembled cell.

electrode, which showed the characteristic lithiation voltage profile of graphite<sup>28</sup> (ESI Fig. S9†). Then, the electrochemical lithium deposition on the lithium metal negative electrode was carried out by charging the cell at a high current density of  $1000 \text{ mA g}^{-1}$  to trigger the lithium dendrite formation and growth. Fig. 4b presents the electrochemical profile of charging, which is followed by discharging. During the charging process, a sudden voltage drop was detected at  $\sim 1100$  seconds, corresponding to approximately  $300 \text{ mA h g}^{-1}$  (denoted by the asterisk in Fig. 4c), which hints at a dendrite penetration into the auxiliary electrode as discussed. Interestingly, after the perturbed cell voltage, the continued charging of the cell did not lead to the prolonged fluctuations of the profile, which is typically observed in the conventional cell after the short-circuit thus failing in charging the cell and aggravating the cell heating.<sup>29,30</sup> Moreover, when continued with the second discharge at  $10 \text{ mA g}^{-1}$ , we did not observe any abnormal discharge behavior.

To elucidate the underlying reason for the perturbed cell voltage denoted with an asterisk, we disassembled the cell after

the second discharge, as shown in Fig. 4c. It revealed that some dark spots are clearly observable on the separator (anode-facing separator) between the lithium electrode and auxiliary electrode, which is the signature of the dendrite short-circuit. More importantly, the auxiliary electrode exhibited yellow domains at the identical region corresponding to the dark spots on the anode-facing separator. This evidently demonstrates that the auxiliary layer was partially lithiated by dendrites, and the region served as a temporary lithium reservoir. On the other hand, the separator (cathode-facing separator) between the graphite positive electrode and auxiliary electrode did not show any noticeable change, maintaining a clean surface, which confirms that the positive electrode was well protected against the risk of short-circuiting. This suggests that without an apparatus to monitor the  $V_2$  of the auxiliary electrode, it is feasible to detect the signals of the dendrite growth in a full cell by simply measuring the full cell voltage, carefully probing the reduction of the overpotential when a high current rate is applied. And, this process is not accompanied by the internal short circuit between the positive and negative electrodes even

with the extended charging process, because the auxiliary electrode continuously scavenges the lithium penetration and serves as an additional lithium reservoir for a certain period of time. This proposes that the concept of the auxiliary electrode for sensing can be applied even for the conventional two-electrode systems, while maintaining its scavenging role, thus retarding the safety hazards.

## Summary

A rechargeable lithium metal battery with reduced safety risk was demonstrated by employing a bifunctional auxiliary electrode. The auxiliary electrode was capable of not only detecting signals of a short-circuit hazard, but also hampering further dendrite growth by scavenging the lithium dendrite in a lithium metal battery. It was confirmed that the auxiliary electrode has no detrimental effect on battery performance with a minimal sacrifice in the energy density and is activated only when batteries are exposed to the risk of short-circuit. Furthermore, the feasibility of the auxiliary sensor in a full cell was verified, showing promise in its applicability to practical batteries. This report provides an interesting new concept of an auxiliary electrode that is capable of sensing and retarding the lithium dendrite growth in lithium metal electrodes and opens up unexplored pathways of using various auxiliary electrode chemistries toward the development of practical lithium metal batteries.

## Materials

Flake-type graphite powder (APS 7–11  $\mu\text{m}$ , 99%) was purchased from Alfa-Aesar. A poly (vinylidene fluoride-co-hexafluoropropylene) binder for the auxiliary electrode and a polyvinylidene fluoride binder for the positive electrode were purchased from Sigma-Aldrich. 300  $\mu\text{m}$  thick Li foil and a battery grade electrolyte (1 M  $\text{LiPF}_6$  in an ethylene carbonate/dimethyl carbonate mixture, volume 1 : 1) were used with a Celgard 2400 separator for cell assembly. Teflon donut rings were inserted to maintain a constant distance between the two electrodes.

## Characterization

The electrochemical performance of the cells was investigated using a potentiostat-galvanostat (WonATech, WBCS 3000, Korea). To measure the ionic conductivity of the electrolyte, electrochemical impedance spectroscopy measurements were carried out over the frequency range of 1.0 GHz to 1.0 Hz (VSP-300, BioLogic Science Instruments, France). The surface morphologies of the lithium metal and auxiliary electrode were examined using scanning electron microscopy (SUPRA 55VP, Carl Zeiss, Germany). *In situ* optical microscopy was performed using an in-house designed cell (ECLIPSE LV150N, Nikon, Japan).

## Conflicts of interest

There are no conflicts to declare.

## Acknowledgements

This work was supported by Project Code. (IBS-R006-A2). S. Moon and O. Tamwattana contributed equally to this work.

## References

- 1 B. Dunn, H. Kamath and J.-M. Tarascon, *Science*, 2011, **334**, 928–935.
- 2 M. Armand and J.-M. Tarascon, *Nature*, 2008, **451**, 652–657.
- 3 J.-M. Tarascon and M. Armand, *Nature*, 2001, **414**, 359–367.
- 4 D. Lin, Y. Liu and Y. Cui, *Nat. Nanotechnol.*, 2017, **12**, 194–206.
- 5 W. Xu, J. Wang, F. Ding, X. Chen, E. Nasybulin, Y. Zhang and J.-G. Zhang, *Energy Environ. Sci.*, 2014, **7**, 513–537.
- 6 P. Bai, J. Li, F. R. Brushett and M. Z. Bazant, *Energy Environ. Sci.*, 2016, **9**, 3221–3229.
- 7 P. Bai, J. Guo, M. Wang, A. Kushima, L. Su, J. Li, F. R. Brushett and M. Z. Bazant, *Joule*, 2018, **2**, 2434–2449.
- 8 D. P. Finegan, M. Scheel, J. B. Robinson, B. Tjaden, I. Hunt, T. J. Mason, J. Millichamp, M. Di Michiel, G. J. Offer, G. Hinds, D. J. L. Brett and P. R. Shearing, *Nat. Commun.*, 2015, **6**, 6924.
- 9 D. P. Finegan, E. Darcy, M. Keyser, B. Tjaden, T. M. M. Heenan, R. Jervis, J. J. Bailey, R. Malik, N. T. Vo, O. V. Magdysyuk, R. Atwood, M. Drakopoulos, M. DiMichiel, A. Rack, G. Hinds, D. J. L. Brett and P. R. Shearing, *Energy Environ. Sci.*, 2017, **10**, 1377–1388.
- 10 K. N. Wood, E. Kazyak, A. F. Chadwick, K.-H. Chen, J.-G. Zhang, K. Thornton and N. P. Dasgupta, *ACS Cent. Sci.*, 2016, **2**, 790–801.
- 11 T. Nishida, K. Nishikawa, M. Rosso and Y. Fukunaka, *Electrochim. Acta*, 2013, **100**, 333–341.
- 12 F. Ding, W. Xu, G. L. Graff, J. Zhang, M. L. Sushko, X. Chen, Y. Shao, M. H. Engelhard, Z. Nie and J. Xiao, *J. Am. Chem. Soc.*, 2013, **135**, 4450–4456.
- 13 Y. Lu, Z. Tu and L. Archer, *Nat. Mater.*, 2014, **13**, 961–969.
- 14 J. Zheng, M. H. Engelhard, D. Mei, S. Jiao, B. J. Polzin, J.-G. Zhang and W. Xu, *Nat. Energy*, 2017, **2**, 17012.
- 15 C.-P. Yang, Y.-X. Yin, S.-F. Zhang, N.-W. Li and Y.-G. Guo, *Nat. Commun.*, 2015, **6**, 8058.
- 16 L.-L. Lu, J. Ge, J.-N. Yang, S.-M. Chen, H.-B. Yao, F. Zhou and S.-H. Yu, *Nano Lett.*, 2016, **16**, 4431–4437.
- 17 H. Lee, D. J. Lee, Y.-J. Kim, J.-K. Park and H.-T. Kim, *J. Power Sources*, 2015, **284**, 103–108.
- 18 G. Zheng, S. W. Lee, Z. Liang, H.-W. Lee, K. Yan, H. Yao, H. Wang, W. Li, S. Chu and Y. Cui, *Nat. Nanotechnol.*, 2014, **9**, 618–623.
- 19 H. Wu, D. Zhuo, D. Kong and Y. Cui, *Nat. Commun.*, 2014, **5**, 5193.
- 20 J. Billaud, F. Bouville, T. Magrini, C. Villeveille and A. R. Studart, *Nat. Energy*, 2016, **1**, 16097.
- 21 S. J. Harris, A. Timmons, D. R. Baker and C. Monroe, *Chem. Phys. Lett.*, 2010, **485**, 265–274.
- 22 P. Maire, A. Evans, H. Kaiser, W. Scheifele and P. Novák, *J. Electrochem. Soc.*, 2008, **155**, A862–A865.

- 23 S. S. Zhang, *J. Power Sources*, 2007, **164**, 351–364.
- 24 T.-H. Cho, M. Tanaka, H. Onishi, Y. Kondo, T. Nakamura, H. Yamazaki, S. Tanase and T. Sakai, *J. Power Sources*, 2008, **181**, 155–160.
- 25 Y.-J. Kim, H. Lee, H. Noh, J. Lee, S. Kim, M.-H. Ryou, Y. M. Lee and H.-T. Kim, *ACS Appl. Mater. Interfaces*, 2017, **9**, 6000–6006.
- 26 M. Rosso, C. Brissot, A. Teyssot, M. Dollé, L. Sannier, J.-M. Tarascon, R. Bouchet and S. Lascaud, *Electrochim. Acta*, 2006, **51**, 5334–5340.
- 27 J. R. Owen, *Chem. Soc. Rev.*, 1997, **26**, 259–267.
- 28 V. A. Sethuraman, L. J. Hardwick, V. Srinivasan and R. Kostecki, *J. Power Sources*, 2010, **195**, 3655–3660.
- 29 X. Liang, Q. Pang, I. R. Kochetkov, M. S. Sempere, H. Huang, X. Sun and L. F. Nazar, *Nat. Energy*, 2017, **2**, 17119.
- 30 L. Li, S. Basu, Y. Wang, Z. Chen, P. Hundekar, B. Wang, J. Shi, Y. Shi, S. Narayanan and N. Koratkar, *Science*, 2018, **359**, 1513.